Electronic Supplementary Information for: Footprints of atomic-scale features in plasmonic nanoparticles as revealed by Electron Energy Loss Spectroscopy

Mattin Urbieta,[*,†,‡,¶] Marc Barbry,[§,¶] Peter Koval,[‖] Alberto Rivacoba,[¶] Daniel Sánchez-Portal,[‡,¶] Javier Aizpurua,[¶,⊥,#] and Nerea Zabala[*,‡,¶,⊥]

†*Matematika Aplikatua Saila, Gipuzkoako Ingeniaritza Eskola (Eibarko Atala), University of the Basque Country (UPV/EHU), 20018 Eibar, Spain.*

‡*Material Physics Center CSIC - UPV/EHU, Paseo Manuel de Lardizabal 5, Donostia-San Sebastian, Gipuzkoa 20018, Spain.*

¶*Donostia International Physics Center (DIPC), Paseo Manuel de Lardizabal 4, Donostia-San Sebastian, Gipuzkoa 20018, Spain.*

§*Centro de Física de Materiales CSIC - UPV/EHU, Paseo Manuel de Lardizabal 5, Donostia-San Sebastian, Gipuzkoa 20018, Spain.*

‖*Simune Atomistics S.L., Avenida de Tolosa 76, Donostia-San Sebastian 20018, Spain.*

⊥*Department of Electricity and Electronics, FCT-ZTF, University of the Basque Country (UPV/EHU), Barrio Sarriena z/g, Leioa, Bizkaia 48940, Spain.*

#*Ikerbasque, Basque Foundation for Science, Bilbao, Bizkaia 48011, Spain*

E-mail: mattin.urbieta@ehu.eus; nerea.zabala@ehu.eus

SI1 Nanoparticle geometries considered within BEM

In this work, we have used a recently developed implementation of EELS calculations within *ab initio* atomistic time-dependent density functional theory (TDDFT), based on the Linear Combination of Atomic Orbitals (LCAO)[1,2] of the Kohn Sham (KS) orbitals $\Psi_n(\mathbf{r})$ within the SIESTA[1,3–5] program. We have calculated within such framework the EEL probability for Na_{380} nanoclusters [Fig. SI1(a)]. Such nanocluster and its geometrical features have been addressed within a Boundary Element Method (BEM)[6] calculations by three different NP shapes. The regular icosahedron (radius of the enclosing sphere $a = 1.85$ nm) plotted in Fig. SI1(b) mimics the atomistic shape of the nanocluster, for which the crystallographic features, such as vertices, edges and facets, are well defined. The geometry labelled as irregular icosahedron used within BEM [Fig. SI1] is built from an isosurface of the ground state electron charge density of the atomistic cluster calculated within density functional theory DFT. We use an isosurface with an electron density threshold value, isovalue of $n_e = 0.00169\, e/\text{Å}^3$,[7] from the ground state charge density of the cluster in the absence of any external perturbation (which is an approximation of the atomistic nanocluster's *surface*). The volume of the resulting continuous NP used in the BEM calculations is equivalent to 380 Na atoms with atomic radius $r_s \sim 2.18$ Å. This value slightly larger to the Wigner-Seitz radius $r_s = 2.08$ Å corresponding to the plasma frequency of Na, $\omega_p = 6.04$ eV, used in the classical dielectric BEM calculations. The larger size can be considered to be due to a certain spillage of electrons to the vacuum, making the NP effectively larger. This shape captures the smoother shape of the NP due to the electron spill-out and limited size of the NP, for which the edges and facets are no longer so well defined as compared to the regular icosahedron.

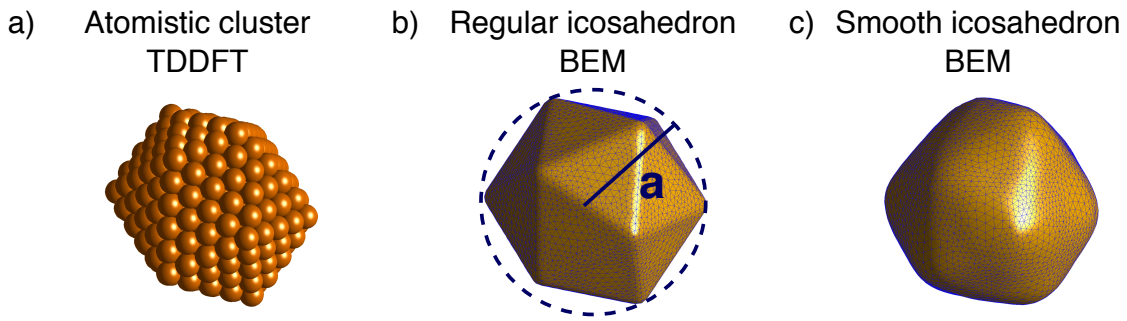

Figure SI1: a) Atomistic Na_{380} cluster used in TDDFT calculations, b) regular icosahedron with enclosing radius a used in BEM calculations, and c) smooth icosahedron (obtained from the ground state isosurface calculated within DFT of the atomistic cluster) used in BEM calculations.

SI2 Dependence of EEL spectra on the kinetic energy of the electron beam and relativistic effects

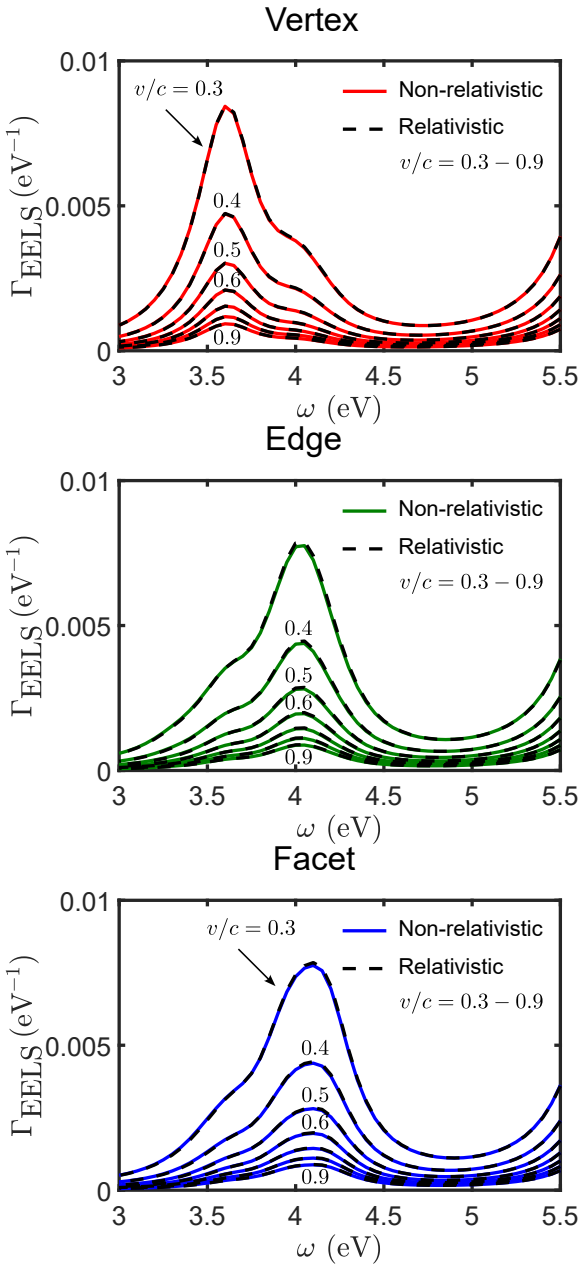

Figure SI2: lectron energy loss spectra as a function of the electron beam velocity, $v/c = 0.3 - 0.9$, calculated within the non-relativistic (solid lines) and relativistic (dashed lines) formalisms for the smooth icosahedron and a) vertex, b) edge and c) facet trajectories. See Fig. 3 of the main text for details about trajectories.

We show in Fig. SI2 the EEL spectra calculated for the irregular icosahedron as probed

by central electron beam trajectories with electron velocities in the range $v/c = 0.3 - 0.9$. As explained in the main text, for small NPs ($\omega_p a/c < 0.2$) the relativistic effects can be safely neglected, as shown by these results. For the velocities considered in our calculations, the only visible change to the spectra is an increase in intensity with decreasing velocities/kinetic energies. To excite odd l-modes kinetic energies down to a few keV are required (not shown in Fig. SI2).

SI3 Quantitative comparison between classical quantum models

In order to quantify the accuracy of the BEM models with respect to the TDDFT results we propose a figure of merit (FOM) based on the energy shifts of the plasmonic modes calculated within the different models. Taking as a reference the TDDFT results, and inspired by the definition of the standard error of estimation, we define the following FOM:

$$\mathrm{FOM} = \sqrt{\frac{\sum_{i=1}^{n}(\omega_{i,\mathrm{TDDFT}} - \omega_{i,\mathrm{BEM}})^2}{n}}, \tag{1}$$

where $\omega_{i,\mathrm{TDDFT}}$ and $\omega_{i,\mathrm{BEM}}$ are the i-th mode calculated within TDDFT and BEM, respectively, and n is the total number of modes used to calculate it. The values obtained by considering the three peaks observed for the vertex, edge and facet trajectories in TDDFT [Fig. 2 in the main text] for the NP shapes considered in our BEM calculations [Figs. 3 and 4 in the main text] are: $\mathrm{FOM}_{\mathrm{regular}} = 0.156$ eV, $\mathrm{FOM}_{\mathrm{smooth}} = 0.132$ eV, and, $\mathrm{FOM}_{\mathrm{sphere}} = 0.323$ eV.

SI4 Charge density distributions for axial trajectories calculated within BEM

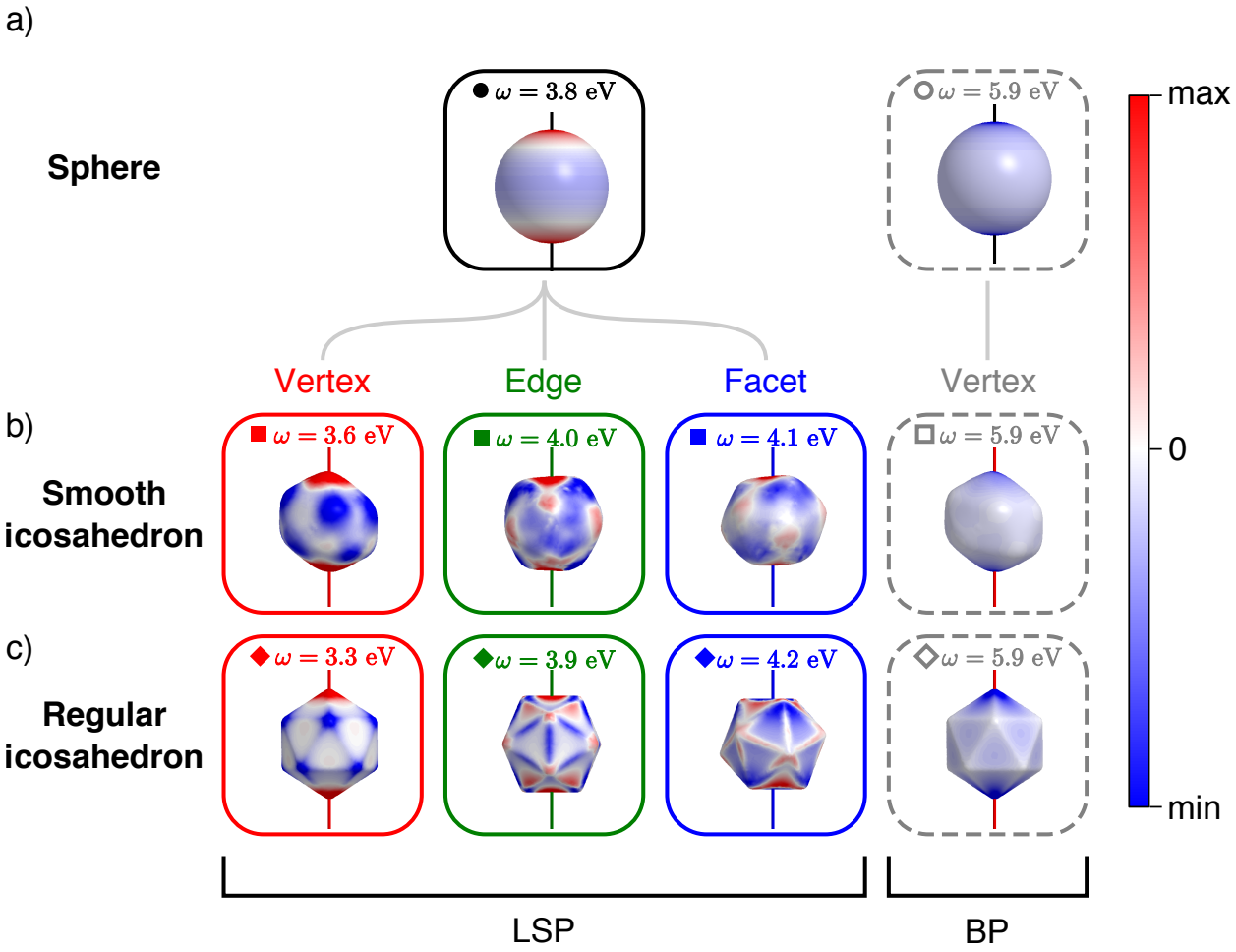

Figure SI3: Side view of charge density plots representing the LSP modes highlighted with squares in Fig. 2(a) and with diamonds in Fig. 2(b) as calculated with BEM for a) a spherical Na NP of radius a =1.85 nm, b) for a smooth icosahedral NP and c) for a regular icosahedral NP.

SI5 EELS logarithmic scale

Fig. SI4 shows the same EELS spectra plotted in Fig. 5(c) of the main text in a logarithmic scale. Confined Bulk Plasmons (CBPs) are excited even for external trajectories with impact parameters much larger than the size of the nanoparticle, although their intensity is almost two orders of magnitude smaller than the intensity of the LSPs, which makes them imperceptible within a linear scale, and evidences the difficulty to detect them experimentally for external trajectories.

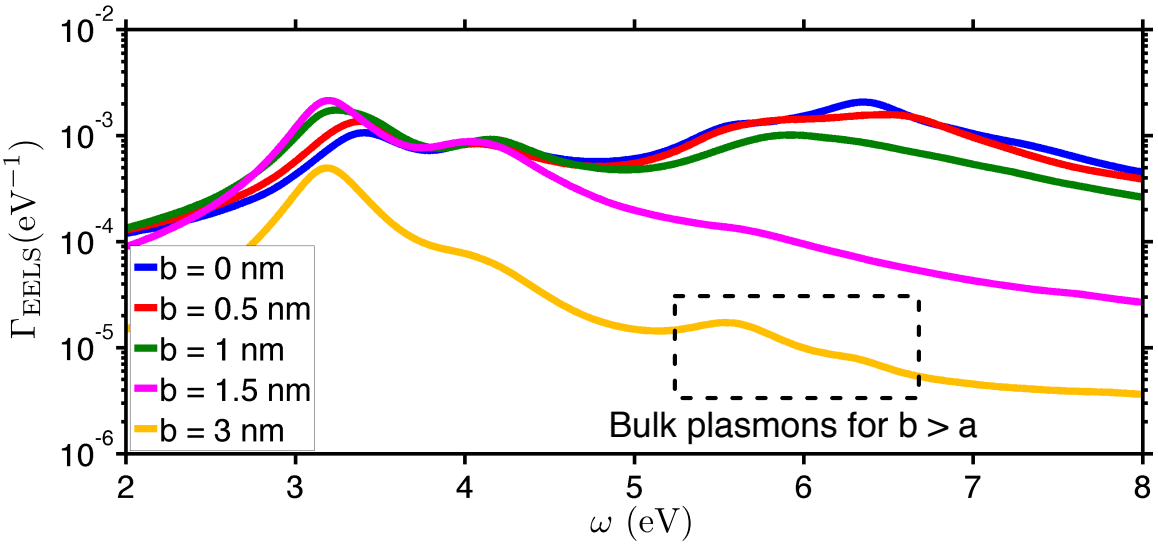

Figure SI4: EEL spectra in logarithmic scale for impact parameters $b = 0$ nm (blue line), $b = 0.5$ nm (red line), $b = 1$ nm (green line), $b = 1.5$ nm (magenta line), and $b = 3$ nm (amber line) for the "near-facet" trajectory (see Fig. 5(b-c) of the main text). CBPs are excited even for $b = 3$ nm (external trajectory), although they are not perceptible if a linear scale is used.

SI6 Orientation dependence of EEL spectra for NP scanning simulations within atomistic TDDFT

In order to check the orientation dependence of the EEL spectra of atomistic NPs scanned by electron beams with changing impact parameter, we selected two other electron trajectory sets related to different orientations: (i) in Fig. SI5(a) we show the orientation of the atomistic NP and the electron trajectory set labelled as "near-edge" that corresponds to electron trajectories parallel to the closest edge (highlighted in cyan) of the NP; (ii) the electron trajectories set labelled as "near-vertex" are plotted in Fig. SI5, and correspond to a set of electron trajectories perpendicular to two opposing vertices (highlighted in cyan) and in-plane with one of the edges formed by the closest vertex to the trajectory.

The color maps of the EEL spectra in Figs. SI5(c,d) corresponding to the near-edge and near-vertex electron trajectories, respectively, share some similarities with the results

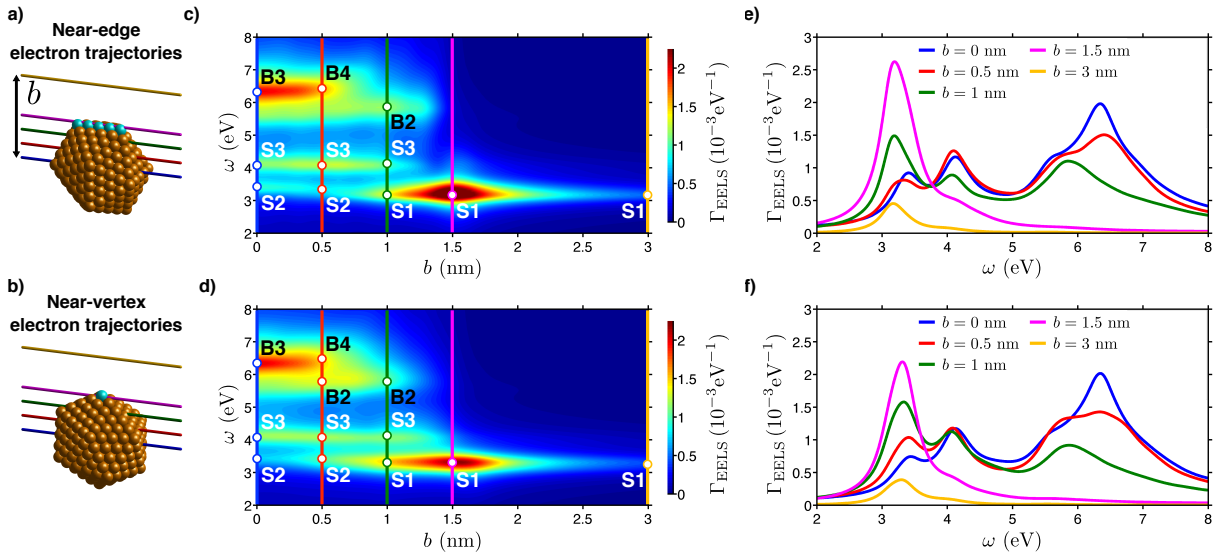

Figure SI5: Trajectory sets are defined for specific orientations of the atomistic cluster related to the trajectories passing near crystallographic features highlighted in cyan and labelled as a) near-edge and b) near-vertex. Color maps of EEL spectra as a function of electron impact parameter b, for c) near-edge, and d) near-vertex electron trajectories, calculated using atomistic TDDFT for a Na nanocluster. The peaks corresponding to different plasmon modes are highlighted by bullet points and labelled as surface (S) or bulk (B) modes. e,f) EEL spectra from (c,d), respectively, for impact parameters $b = 0$ nm (blue line), $b = 0.5$ nm (red line), $b = 1$ nm (green line), $b = 1.5$ nm (magenta line), and $b = 3$ nm (amber line).

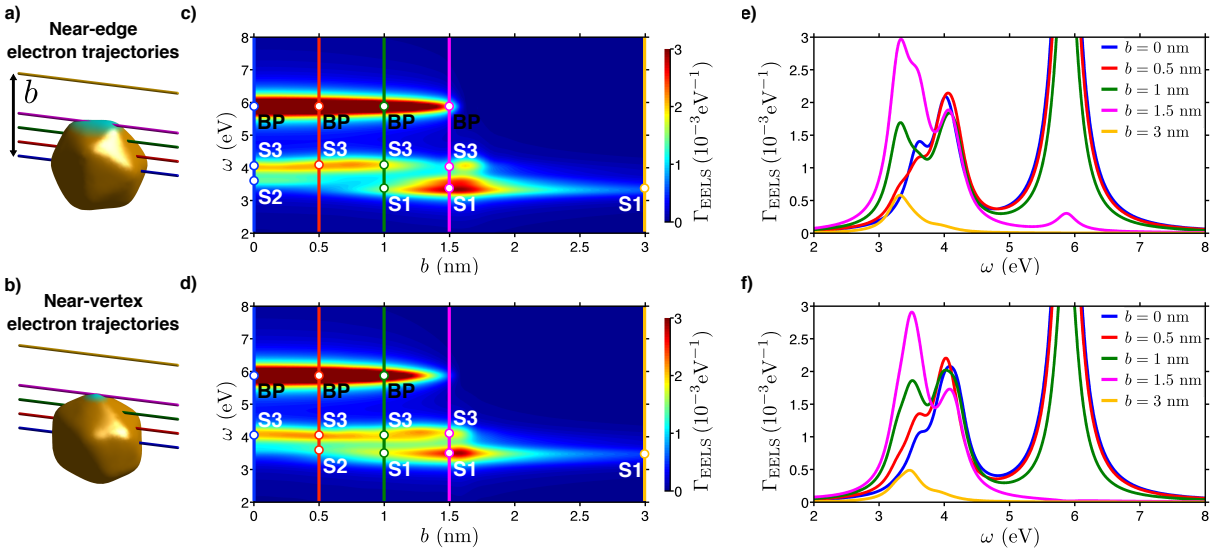

Figure SI6: Trajectory sets are defined for specific orientations of the NP related to the trajectories passing near crystallographic features highlighted in cyan and labelled as a) near-edge and b) near-vertex. Color maps of EEL spectra as a function of electron impact parameter b, for c) near-edge, and d) near-vertex electron trajectories, calculated using BEM for a Na NP. The peaks corresponding to different plasmon modes are highlighted by bullet points and labelled as surface (S) or bulk (B) modes. e,f) EEL spectra from (c,d), respectively, for impact parameters $b = 0$ nm (blue line), $b = 0.5$ nm (red line), $b = 1$ nm (green line), $b = 1.5$ nm (magenta line), and $b = 3$ nm (amber line).

for the "near-facet" trajectories [Fig. 5(b) of the main text], such as the excitation of the dipolar plasmon (S1) for external trajectories, and the overall distribution of the peaks. Nevertheless, there are some differences regarding the excitation of HOP (S3) modes and the relative intensity of the peaks. Such differences are better appreciated by comparing Fig. 5(c) of the main text and Figs. SI5(e,f), which show EEL spectra selected for impact parameters $b = 0$, 0.5, 1, 1.5 and 3 nm and corresponding to the electron trajectories sketched in Fig. 5(a) of the main text and Figs. SI5(a,b) for the near-facet, near-edge and near-vertex electron trajectories, respectively. For instance, for the trajectory labeled as "near-edge" [Fig. SI5(e), almost no excitation of the S3 modes is observed for grazing incidence and the relative intensities of modes S2 and S3 for penetrating trajectories are different as among the different electron trajectory sets. On the other hand, CBPs show seemingly no strong dependence on the NP's orientation.

As explained in the main text, we calculate the impact parameter dependent EEL spectra

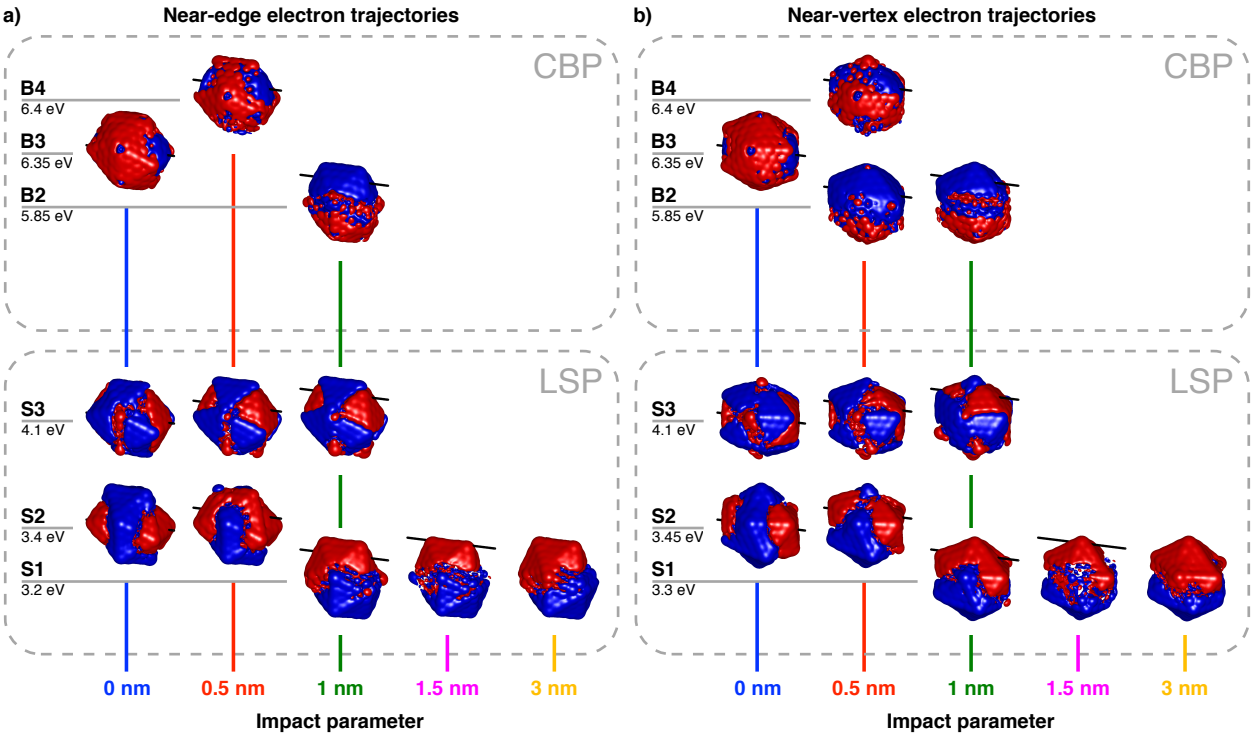

Figure SI7: Isosurfaces of the imaginary part of the charge density corresponding to the a) near-edge and b) near-vertex electro trajectories corresponding to the peaks highlighted, respectively, in Figs. SI5(c,d), calculated using TDDFT for impact parameters $b = 0, 0.5, 1, 1.5, 3$ nm.

within BEM for a smooth icosahedron for the near-edge and near-vertex electron trajectory sets, depicted in Figs. SI6(a,b). The color maps of the EEL spectra corresponding to each electron trajectory set are shown in Figs. SI5(c,d), and EEL spectra selected for impact parameters $b = 0$, 0.5, 1, 1.5 and 3 nm are shown in Figs. SI6(e,f). Overall the BEM results reproduce the trends observed in the TDDFT results corresponding to the LSPs, although there is a characteristic overestimation of the HOP modes (labelled as S3) due to non-local effects (details in the main text), which produces some differences in the shape of the spectra and intensity of the peaks. Indeed, some peaks present in the the spectra calculated within TDDFT are not clearly discernible in the BEM results, which explains the absence of certain peaks in the LSP spectra in Figs. SI6(b,c). As expected, BEM calculations are unable to reproduce the impact parameter dependence of CBPs.

The subtle differences observed in the spectra for different orientations of the NPs emerge clearer in the induced charge density distributions. In Fig. SI7 we plot the isosurfaces

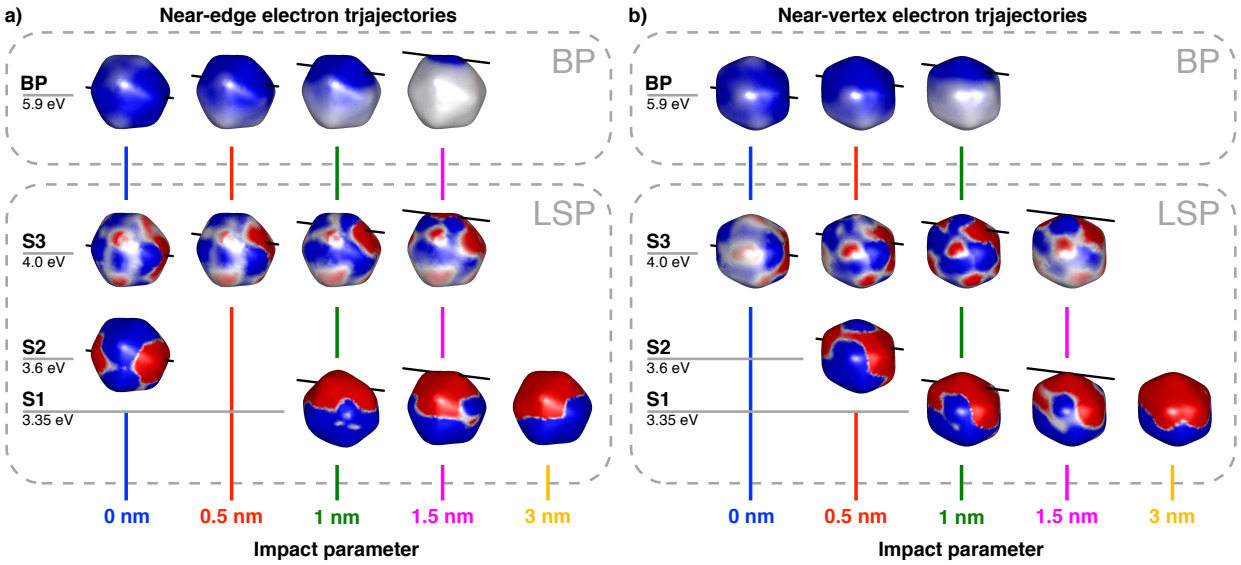

Figure SI8: Induced surface charge density distributions corresponding to the a) near-edge and b) near-vertex electro trajectories corresponding to the peaks highlighted, respectively, in Figs. SI5(c,d), calculated using TDDFT for impact parameters $b = 0, 0.5, 1, 1.5, 3$ nm.

obtained from the induced charge density calculated within atomistic TDDFT for the near-edge and near-vertex electron trajectories and corresponding to the main excitations observed in Figs. SI5(c,d) for impact parameters $b = 0$, 0.5, 1, 1.5, 3 nm. The patterns observed for the charge densities show a clear orientation and impact parameter dependence of the charge density distributions for the LPPs. On the other hand, CBPs do not show any apparent dependence on the orientation of the NPs (although they do on the impact parameter), and thus in principle it should be possible to address them properly within models that consider the NPs to be spherical.

The charge density distributions plotted in Fig. SI8 correspond to the main excitations observed in Figs. SI5(c,d) for impact parameters $b = 0$, 0.5, 1, 1.5, 3 nm and near-edge and near-vertex electron trajectories calculated for the smooth icosahedron within BEM. The results show that the local classical approach can reproduce the induced charge distributions corresponding to the LSPs and can capture the atomic-scale features and shape effects properly if an accurate shape resembling the landscape of the electron density is used.

References

1. Koval, P.; Barbry, M.; Sánchez-Portal, D. PySCF-NAO: An efficient and flexible implementation of linear response time-dependent density functional theory with numerical atomic orbitals. *Computer Physics Communications* **2019**, *236*, 188–204.

2. Foerster, D. On an "interaction by moments" property of four center integrals. *arXiv:physics/0612187* **2006**,

3. Sánchez-Portal, D.; Ordejón, P.; Artacho, E.; Soler, J. M. Density-functional method for very large systems with LCAO basis sets. *International Journal of Quantum Chemistry* **1997**, *65*, 453–461.

4. Soler, J. M.; Artacho, E.; Gale, J. D.; García, A.; Junquera, J.; Ordejón, P.; Sánchez-Portal, D. The SIESTA method for ab initio order-N materials simulation. *Journal of Physics: Condensed Matter* **2002**, *14*, 2745–2779.

5. Barbry, M. Plasmons in Nanoparticles: Atomistic Ab Initio Theory for Large Systems. Ph.D. thesis, University of the Basque Country, UPV-EHU, San Sebastian, 2018.

6. Hohenester, U. Simulating electron energy loss spectroscopy with the MNPBEM toolbox. *Computer Physics Communications* **2014**, *185*, 1177–1187.

7. Marchesin, F.; Koval, P.; Barbry, M.; Aizpurua, J.; Sánchez-Portal, D. Plasmonic Response of Metallic Nanojunctions Driven by Single Atom Motion: Quantum Transport Revealed in Optics. *ACS Photonics* **2016**, *3*, 269–277.